Removal of Various Heavy Metals by Sewage Sludge Immobilized Onto Rod-type Chitosan Biosorbent

Ji Hae Seo
Yonsei University
Namgyu Kim
Yonsei University
Munsik Park
Yonsei University
Donghee Park (dpark@yonsei.ac.kr)
Yonsei University

Research Article

Keywords: sludge, biosorption, chitosan, arsenic, mechanism

Posted Date: March 6th, 2021

DOI: https://doi.org/10.21203/rs.3.rs-266882/v1

Removal of various heavy metals by sewage sludge immobilized onto rod-type chitosan biosorbent

Ji Hae Seo[1], Namgyu Kim[1], Munsik Park, Donghee Park*

Department of Environmental Engineering, Yonsei University, 1 Yonseidae-gil, Wonju, 26493, Republic of Korea

[1] These authors contributed equally.

* **To whom all correspondence should be addressed.**

E-mail address: dpark@yonsei.ac.kr; Tel.: +82 33 760 2435; Fax: +82 33 760 2571.

Abstract

The potential use of wastewater sludge as a biosorbent for removing various metals and metalloids from aqueous solutions was examined. The sludge was immobilized by chitosan into rods to enhance the sorption capacity and solid-liquid separation ability. An optimum condition of rod-type chitosan-immobilized sludge (RCS) was selected from possibility of produced biosorbent and the removal efficiency of As(V). The optimal sludge and chitosan content and RCS thickness was 6.0%, 4.0% and 0.2-0.3 mm, respectively. The experiments targeted cations(Cd(II)) and anions(As(V), Cr(VI), and Mn(VII)). Pseudo-first-order and pseudo-second-order models adequately described kinetics models and Langmuir and Freundlich models described isotherm models for RCS, which showed higher adsorption ability for anionic metals over cationic metals. The results indicate that electrostatic attraction or ion exchange is the most important mechanism for metal/metalloid adsorption, except in the case of Mn(VII), for which an adsorption-coupled reduction mechanism is suggested.

Keywords: sludge; biosorption; chitosan; arsenic; mechanism;

1. Introduction

During the development of industry, the presence of toxic heavy metal contamination of the environment is a source of serious concern. Due to their harmful effects on human health, finding methods to remove heavy metals is of great importance. Chemical precipitation, ion exchange, evaporation, electroplating and membrane processes are common commercial methods for removing excessive concentrations of heavy metals from aqueous solutions [1, 2]. However, these methods can be expensive and inefficient and generate chemical sludge. New environmentally friendly technologies for removing heavy metal ions from wastewater are urgently needed.

Recently, biosorption has been suggested as a possible alternative to conventional methods of heavy metal removal [3]. The main advantages of biosorption are reusability, low operating costs, and no production of toxic secondary compounds. Biosorbents, the adsorbents used in biosorption, are prepared from various biomasses such as algae, aquatic plants, moss, and bacteria, all of which can be difficult to produce in large quantities. Many researches have been carried out to produce biosorbent using wastewater sludge which has no limitation on the production amount [4-7]. The use of wastewater sludge for biosorbent offered not the naturally abundant but also no requirement of nutrients, and easy availability. Even though it has merits, it often suffers several drawbacks using raw wastewater sludge. The most important limitations include solid-liquid separation problems, possible biomass swelling and inability to regenerate/reuse [3, 8]. To overcome this drawback, wastewater sludge therefore needs to be immobilized. Chitosan, sodium alginate, polysulfone, polyacrylamide, and polyurethane have been used as matrix materials for immobilization of biosorbents [9, 10]. Special attention has been given to polysaccharides and natural polymers such as chitosan, which is an emerging matrix materials for immobilizing biomass [11].

In this study, sewage-sludge waste was used as a raw material for the manufacture of

biosorbents for the removal of heavy metals from aqueous solutions by batch biosorption experiments. To facilitate sold-liquid separation, sludge was immobilized by chitosan, which is known as a common, inexpensive, and environmentally friendly matrix material. Fourier-transform infrared spectroscopy (FTIR) analysis and total organic carbon (TOC) measurements were taken to confirm immobilization strength and characteristics. Kinetic and isotherm experiments were conducted to evaluate biosorption rates and the capacity of the biosorbent to remove various metals.

2. Materials

2.1. Preparation of the rod-type biosorbent

The raw material used in the experiments was a biochemical sludge from a biological wastewater treatment plant in Yonsei University, Korea. Average sludge comprised 15 ± 5% total solids and 70 ± 5% volatile solids/total solids. The immobilization process began with 2–6% (w/v) activated sludge (ignoring moisture) stirred in distilled water. After mixing, a 3–6% (w/v) solution of chitosan and 5% acetic acid (v/v) was added by continuous stirring with a mechanical stirrer at 160 rpm for 24 h. The mixture was extruded through syringes (0.2–0.3 mm, 0.5–0.6 mm, 0.8–0.9 mm and 1.0–1.2 mm diameter) into 2 M sodium hydroxide. The resultant rod-type biosorbent was kept in a polymerizing medium for 4 h. To compare biosorbent types, we also produced bead-type biosorbents with the same process. Biosorbents were washed in distilled and deionized water to leach out excess solvents and then freeze-dried. The dried biosorbent rods were stored in a desiccator until used in the experiments.

2.2. Reagents

Chitosan (75–85% acetylation degree, molecular weight: 200–800 kDa) was supplied by Sigma-Aldrich (USA). Acetic acid (purity > 99%) was purchased from Duksan (Korea). Pure analytical grade As(V), Cd(II), Cr(VI), and Mn(VII) solutions were prepared by dissolving solid $Na_2HAsO_4 \cdot 7H_2O$ (Sigma-Aldrich, USA), $Cd(NO_3)_2 \cdot 4H_2O$ (Sigma-Aldrich, USA), $K_2Cr_2O_7$ (Junsei, Japan), and $KMnO_4$ (Samchun, Korea) in distilled water. All chemicals used in this study were of analytical grade. The pH of the solutions was adjusted by adding sodium hydroxide (Samchun, Korea) or hydrogen chloride (Samchun, Korea) solutions.

2.3. Batch adsorption studies

The kinetics and isothermal removal of As(V), Cd(II), Cr(VI), and Mn(VII) from aqueous solutions by biosorbent rods was observed in 230 mL plastic bottles. The equilibration (shaking) time was 6 h in contact with 200 mL of the wastewater. The bottles were agitated in a shaker at 200 rpm at room temperature. In the kinetics experiment, 2.0 g/L of each biosorbent was put into contact with 50 mg/L of each metal or metalloid solution. All solutions were adjusted to pH 5.5. Isotherm experiments were carried out at various metal concentrations, ranging from 50 mg/L to 1500 mg/L. In all batch experiments, the solution pH was maintained at the desired value using 1 M HCl and 1 M NaOH solutions. The amount of metal or metalloid adsorbed on the biosorbent, q (mg/g), was calculated using the mass balance equation

$$q\ (mg/g) = \frac{(C_0 - C_e)V}{m} \quad (1)$$

where C_0 and C_e are the initial and equilibrium concentrations (mg/L), respectively, V is the working volume (L), and m is the weight of the biomass (g). All biosorption experiments

were performed in triplicate, with an error rate of less than 5%. Mean values were used for kinetic and isotherm experimental data.

2.5. Analytical methods

TOC of the solution was measured using a TOC analyzer (TOC-VCPH/CPN, SHIMADZU, Japan). Total nitrogen (TN) and total phosphorous (TP) were determined using a test kit (C-MAC. Co., Korea). An infrared spectrum of the biosorbent with an FTIR spectrometer (Vertex 70, Bruker, USA). An inductively coupled plasma-optical emission spectrometer (ICP/IRIS, Thermo Jarrell Ash Co., USA) was used to analyze total metals after being filtered through a 0.20 μm membrane. The Cr(VI) concentration was determined by spectrophotometric analysis at 540 nm according to a standard method using 1,5-diphenylcarbazide. The pink color of Mn(VII) was analyzed at 525 nm to measure its concentration.

3. Results and discussion

3.1. Characteristics of chitosan-immobilized biosorbent

Because the activated sludge was composed of bacteria and protozoa, a biosorbent made directly from the sludge may unintentionally contaminate a water system [12]. An immobilization technique can address this problem. In this study, biosorbents were prepared by an immobilization technique using chitosan. While much research in recent years has focused on immobilization using chitosan, few studies have attempted to evaluate immobilization performance. We tested the performance of immobilization through analysis of TOC released from the biosorbent during pretreatment with deionized and distilled water. TOC released from immobilized biosorbents was much lower than TOC released from raw

140 biosorbent. In addition, TN and TP, which are indicators of pollution, were also found to be
141 less eluted (Table 1), suggesting that immobilization can alter the properties of a biosorbent,
142 including surface functional groups. In particular, a fuctional groups on the surface often
143 changes after immobilization. To determine the nature of functional group change, raw
144 biosorbents and chitosan-immobilized biosorbents were examined using FTIR analysis (SI
145 Fig. 1). The spectra of the raw biosorbent and chitosan-immobilized biosorbents displayed
146 many absorption peaks. A broad and strong band in the 3600–3200 cm^{-1} region was
147 associated with N-H and O-H stretching vibrations in amine and hydroxyl groups [13]. Two
148 spectra also displayed absorption peaks at 1650 cm^{-1} and 1750 cm^{-1} relevant to the stretching
149 band of the carboxyl double bond in the carboxyl functional group [14]. The phosphate group
150 also observed everything (1150 cm^{-1} [=O stretching] and 1050 cm^{-1} [POH stretching and/or
151 POC stretching]) [15]. After the chitosan immobilized the biomass, the FTIR spectrum
152 showed some peak changes (SI Fig. 1). The band at 3378 cm^{-1} broadened because of the
153 large number of amine groups in chitosan. Amine group biosorption sites played the most
154 significant role in anionic metal removal [16]. The FTIR results show that chitosan-
155 immobilized biomass was expected to remove anionic metal more effectively than raw
156 biomass [17].
157
158 ***3.2. Optimization of rod-type biosorbent modification conditions***
159 The biosorbent shape, sludge content, chitosan content, and diameter of the biosorbent
160 were manipulated to optimize biosorbent preparation.
161
162 ***3.2.1 Effect of biosorbent shape***
163 A kinetics study was conducted to determine the effect of immobilization and biosorbent
164 shape on adsorption. Experiments using raw sludge (RS), bead-type of chitosan-immobilized

sludge (BCS), and rod-type chitosan-immobilized sludge (RCS) were performed to evaluate the contact time required to reach equilibrium. Chitosan is a biopolymer with a high nitrogen content that confers an adsorption ability for anionic metal ions. As(V) was used to evaluate the performance of each biosorbent. Figure 1(a) exhibits the As(V) removal of RS, BCS, and RCS as a function of contact time at a pH of 5.5. BCS and RCS delivered an As(V) removal efficiency that was 2–3 times higher than that of RS. This result can be attributed to the presence of amine groups on the biosorbent [18].

3.2.2 Effect of material content in biosorbent

The amounts of sludge and chitosan were important variables affecting sorption performance. Figure 1(b) shows the effects of sludge on As(V) removal onto RCS. The sludge content influenced the biomass surface, affecting the capacity of the biomass for As(V) biosorption. For finer details, we compared adsorption results through pseudo-first-order and pseudo-second-order kinetics modeling. These models were employed to investigate the adsorption dynamics of pollutants onto the biosorbents in relation to time and to estimate the rate of the process. They can also shed light on biosorption mechanisms and potential rate-controlling steps, which may include mass transport and chemical reaction processes [19]. The pseudo-first-order equation is:

$$q_t = q_e(1 - e^{-k_1 t}) \quad (2)$$

where q_e is the amount of adsorbate adsorbed (mg/g) at equilibrium, q_t is the amount of adsorbate adsorbed (mg/g) at time t (min) and k_1 (min^{-1}) is the rate constant.

The pseudo-second-order equation is usually associated with the situation in which the rate of direct adsorption or desorption controls the overall sorption kinetics, and typically

describes the removal behavior of metals [20, 21]. An integrated form of the pseudo-second-order equation can be expressed as:

$$\frac{t}{q_t} = \frac{1}{k_2 \cdot q_e^2} + \frac{t}{q_e} \quad (3)$$

or

$$\frac{q_t}{t} = \frac{h}{1+k_2 q_e t} \quad (4)$$

where h (g/mg·h) is the initial sorption rate and k_2 (g/mg·h) is the rate constant. From the equations of the different obtained the equilibrium metal sorption, values for the rate constant, initial sorption rate, and coefficients were calculated and are presented in Table 2. In the case of equilibrium uptake, q_e, removal increases with increasing sludge ratio in RCS. When comparing the rate constant and initial sorption rate, RCS with 4.0% sludge shows the fastest rate. From these results, it can be seen that 4.0% was satisfied in terms of speed, but 6.0% was the optimal adsorption amount. To increase adsorption, we attempted to produce an adsorbent containing more than 6.0% sludge. However, producing the biosorbent in this manner proved problematic. We therefore set the optimum sludge content at 6.0% of RCS, which showed the maximum amount and has the benefit environmental load.

The effect of the chitosan content in RCS on biosorption of As(V) is shown in Fig. 1(c). The data used in Equations 2–4 are presented in Table 2. A chitosan content of 6.0% in RCS showed higher removal of As(V) compared with other RCS. The higher removal may be due to the effect of As(V) on the chitosan amine group in RCS. Comparing correlation coefficients (R^2), the pseudo-second-order kinetic model was a better fit in describing the biosorption kinetics of studied heavy metals onto RCS. It was assumed that the As(V) adsorption process was chemisorption involving valency forces through sharing or the

214 exchange of electrons between the RCS and As(V) as covalent forces [22]. This facilitated
215 the electrostatic attraction of As(V) ions toward RCS, leading to an increase in biosorption.
216 However, when the equilibrium uptake, rate constant, and initial sorption rate values of As(V)
217 were examined, the effect of chitosan in RCS was not as dramatic, considering the
218 economical manufacture of biosorbent focuses on RCS with sludge and chitosan contents of
219 6.0% and 4.0%, respectively.
220
221 ***3.2.3 Effect of biosobent size***
222 Biosorbent diameter size is an important controlling parameter of the biosorption
223 process. The effect of RCS diameter size on As(V) biosorption was studied using samples of
224 four biosorbents with average diameters of 0.2–0.3, 0.5–0.6, 0.8–0.9 and 1.0–1.2 mm, and
225 sludge and chitosan contents of 6.0% and 4.0%. The results are presented in Fig. 1(d).
226 Equilibrium uptake values showed similar values (Table 2). However, the rate constant and
227 initial sorption rate decreased when the biosorbent diameter increased from 0.2–0.3 to 1.0–
228 1.2 mm. The higher biosorption with smaller RCS diameters may be attributed to the fact that
229 RCS with smaller diameter has greater surface area. Therefore, an RCS diameter size of 0.2–
230 0.3 mm was selected for experimental purposes.
231
232 ***3.3. Adsorption study***
233 ***3.3.1 Kinetics***
234 Figure 2 shows the kinetics of metalloid/metal adsorption onto RCS by batch contact
235 time. Equilibrium times were different among the metalloids/metals. For Cd(II) ions,
236 equilibrium states were reached after 1 h. The As(V) and Cr(VI) sorptions were achieved
237 after 3 and hours of contact time, respectively. The Mn(VII) sorptions were finished after 6 h.
238 Table 3 shows that the pseudo-second-order equation, which agrees that chemisorption is the

239 rate-controlling mechanism, was able to better describe the adsorption of As(V), Cd(II),
240 Cr(VI) and Mn(VII) onto RCS. By comparing the amount of metals adsorbed at equilibrium,
241 the following order was obtained: Mn(VII) > Cr(VI) > As(V) > Cd(II). While Mn(VII) was
242 completely removed, sorption of Mn(VII) did not fit the kinetics models. The Mn(VII)
243 removal mechanism is recognized to differ from that of other metals. To examine the
244 Mn(VII) removal characteristics of RCS, total Mn concentrations were investigated (SI Fig.
245 2). After complete Mn(VII) removal, Mn remained in the aqueous phase. It can therefore be
246 concluded that the Mn(VII) removed from aqueous phase was reduced to other species of Mn
247 [23]. Despite the fact that Cd(II) ions, as representative metal cations, were more weakly
248 adsorbed than the other metals, their removal showed the fastest kinetics. It appears that
249 Cd(II) reacted strongly with other functional groups. In general, it is known that the carboxyl
250 group is involved in the adsorption of Cd (II) [24, 25]. The adsorption of Cd (II) was weakly
251 adsorbed because it was decreased carboxyl group in the RCS compared the raw sludge (SI
252 Fig. 1).
253
254 ***3.3.2 Isotherms***
255 Biosorption isotherms can represent the interaction between a biosorbate and biosorbent,
256 and provide information about the distribution of the biosorbate between the liquid and solid
257 phases at several equilibrium concentrations. Isotherm modeling is therefore important for
258 biosorption data interpretation and prediction [7, 26]. In this study, isotherm models of
259 Freundlich and Langmuir were used to evaluate biosorption equilibrium data. Freundlich and
260 Langmuir isotherm equations are in the forms of:
261
262 $$q_e = K_F C_e^{1/n} \quad (5)$$
263 and

$$q_e = \frac{q_{max} b C_e}{1 + b C_e} \quad (6)$$

where K_f and n are constants incorporating all parameters affecting the biosorption process in the Freundlich equation and b is the constant related to affinity of the binding sites in the Langmuir equation. In the Freundlich equation, K_F $(L/mg)^{1/n}$ and n (dimensionless) are constants. On average, a favorable adsorption tends to have a n between 1 and 10. In the Langmuir equation, q_{max} is the maximum adsorption capacity (mg/g) and b (L/g) is the isotherm constant.

Langmuir and Freundlich isotherm models were used to interpret the experimental isotherm data of RCS. Model parameters and R^2 values are summarized in Table 3. The sorption experimental data and respective Langmuir and Freundlich isotherms are plotted in Fig. 3(a), (b), (c) and (d) respectively. A linear regression of the experimental results for As(V) and Cr(VI) proved a better fit in Langmuir isotherms. This result can be attributed to the fact that As(V) and Cr(VI) biosorption of RCS was assumed by sorbate, and the equation describing the reaction rate allows for simultaneous adsorption and desorption [27]. When comparing Langmuir parameters values obtained for As(V) and Cr(VI), q_{max} was approximately 42.25 mg As(V) or 70.79 mg Cr(VI) per g of RCS. The values for As(V) from the present study are comparable or considerably greater than other reported sludge sorbents (Table 4). The other metals, Cd(II) and Mn(VII), were well described by the Freundlich equation based on R^2. This difference may be explained by the presence of an operating mechanism other than basic ion exchange, such as specific adsorption-complexation reactions taking place in the adsorption process [28]. As mentioned above, the biosorption mechanism of Mn(VII) was suggested by an adsorption-coupled reduction mechanism.

4. Conclusions

The aim of the present study was to develop a high-performance biosorbent of non-living activated sludge. The incorporation of immobilizing chitosan, which was confirmed by the release of TOC, TN, and TP from the biosorbent during pretreatment with deionized-distilled water wash, may offer an effective method of decreasing metal and metalloid concentrations in wastewater. Comparing experiments for adsorption of As(V), the optimal conditions for biosorption were a rod shape, 4.0% chitosan, and a biosorbent diameter of 0.2–0.3 mm, in contact with 6.0% dried sludge. An investigation of the removal rates of various cationic and anionic heavy metals found that RCS had adsorbed anionic metals more effectively than cationic metals. The maximum biosorption capacities of RCS were determined to be 42.25 mg/g for As(V), 28.69 mg/g for Cd(II), 70.79 mg/g for Cr(VI), and 284.11 mg/g for Mn(VII). The model-fitting results indicate that adsorption-coupled reduction and ion exchange must be involved in the adsorption of the Mn(VII), while ion exchange or electrostatic attraction is the most important mechanism for other metals and metalloids.

Acknowledgments

This work was supported by the BK21 program through the National Research Foundation (NRF) funded by the Ministry of Education of Korea. This work was also partially supported by the Ministry of Education of Korea (2019R1A6A3A01096685)

Author contributions

Ji Hae Seo: Methodology, Experiment

Namgyu Kim: Conceptualization, Writing-Original draft preparation

Munsik Park: Investigation, Methodology

Donghee Park: Project administration, Writing-Review & Editing

Competing interests statement

All authors declare that they have no known competing financial interests or personal relationships that could have appeared to influence the work reported in this paper.

References

1. Fu, F., Wang, Q. Removal of heavy metal ions from wastewaters: A review. *J. Environ. Manage.* **92**, 407-418 (2011).

2. Yaqub, M., Lee, S. H. Heavy metals removal from aqueous solution through micellar enhanced ultrafiltration: A review. *Environ. Eng. Res.* **24**, 363-375 (2019).

3. Park, D., Yun, Y. S., Park, J. M. The past, present, and future trends of biosorption. *Biotechnol. Bioprocess Eng.* **15**, 86-102 (2010).

4. Al-Qodah, Z. Biosorption of heavy metal ions from aqueous solutions by activated sludge. *Desalination* **196**, 164-176 (2006).

5. Maderova, Z., Baldikova, E., Pospiskova, K., Safarik, I., Safarikova, M. Removal of dyes by adsorption on magnetically modified activated sludge. *Int. J. Environ. Sci. Technol.* **13**, 1653-1664 (2016).

6. Ozdemir, S., Turp, S. M., Oz, N. Simultaneous dry-sorption of heavy metals by porous adsorbents during sludge composting. *Environ. Eng. Res.* **25**, 258-265 (2020).

7. Seo, J. H., Kim, N., Park, M., Lee, S., Yeon, S., Park, D. Evaluation of metal removal performance of rod-type biosorbent prepared from sewage-sludge. *Environ. Eng. Res.* **25**, 700-706 (2020).

8. Dai, Y., Zhang, N., Xing, C., Cui, Q., Sun, Q. The adsorption, regeneration and engineering applications of biochar for removal organic pollutants: A review. *Chemosphere* **223**, 12-27 (2019).

9. Lin, X., Wang, L., Jiang, S., Cui, L., Wu, G. Iron-doped chitosan microsphere for As(III) adsorption in aqueous solution: Kinetic, isotherm and thermodynamics studies. *Korean J. Chem. Eng.* **36**, 1102-1114 (2019).

10. Vijayaraghavan, K., Yun, Y. -S. Bacterial biosorbents and biosorption. *Biotechnol. Adv.* **26**, 266-291 (2008).

348 11. Gerente, C., Lee, V. K. C. , Le Cloirec, P., McKay, G. Application of chitosan for the
349 removal of metals from wastewaters by adsorption - Mechanisms and models review. *Crit.*
350 *Rev. Environ. Sci. Technol.* **37**, 41-127 (2007).
351 12. Amrullah, A., Paksung, N., Matsumura, Y. Cell structure destruction and its kinetics
352 during hydrothermal treatment of sewage sludge. *Korean J. Chem. Eng.* **36**, 433-438
353 (2019).
354 13. Altun, T., Ecevit, H. Cr(VI) removal using Fe_2O_3-chitosan-cherry kernel shell pyrolytic
355 charcoal composite beads. *Environ. Eng. Res.* **25**, 426-438 (2000).
356 14. Chen, Q., Zheng, J., Wen, L., Yang, C., Zhang, L. A multi-functional-group modified
357 cellulose for enhanced heavy metal cadmium adsorption: Performance and quantum
358 chemical mechanism. *Chemosphere* **224**, 509-518 (2019).
359 15. Ramrakhiani, L., Majumder, R., Khowala, S. Removal of hexavalent chromium by heat
360 inactivated fungal biomass of *Termitomyces clypeatus*: Surface characterization and
361 mechanism of biosorption. *Chem. Eng. J.* **171**, 1060-1068 (2011).
362 16. Kim, N., Park, M., Yun, Y.-S., Park, D. Removal of anionic arsenate by a bacterial
363 biosorbent prepared from fermentation biowaste. *Chemosphere* **226**, 67-74 (2019).
364 17. Lipatova, I. M., Makarova, L. I., Yusova, A. A. Adsorption removal of anionic dyes from
365 aqueous solutions by chitosan nanoparticles deposited on the fibrous carrier.
366 *Chemosphere* **212**, 1155-1162 (2018).
367 18. Deng, S., Ting, Y.P. Polyethylenimine-modified fungal biomass as a high-capacity
368 biosorbent for Cr(VI) anions: Sorption capacity and uptake mechanisms. *Environ. Sci.*
369 *Technol.* **39**, 8490-8496 (2005).
370 19. Ho, Y. S. Review of second-order models for adsorption systems. *J. Hazard. Mater.* **136**,
371 681-689 (2006).
372 20. Ho, Y. S., McKay, G. Pseudo-second order model for sorption processes. *Process*

373 *Biochem.* **34**, 451-465 (1999).
374 21. Tran, H. N., You, S. -J., Hosseini-Bandegharaei, A., Chao, H. -P. Mistakes and
375 inconsistencies regarding adsorption of contaminants from aqueous solutions: A critical
376 review. *Water Res.* **120**, 88-116 (2017).
377 22. Graillot, A., Bouyer, D., Monge, S., Robin, J. J., Loison, P., Faur, C. Sorption properties
378 of a new thermosensitive copolymeric sorbent bearing phosphonic acid moieties in multi-
379 component solution of cationic species. *J. Hazard. Mater.* **260**, 425-433 (2013).
380 23. Dash, S., Patel, S., Mishra, B. K. Oxidation by permanganate: synthetic and mechanistic
381 aspects. *Tetrahedron* **65**, 707-739 (2009).
382 24. Kim, N., Park, M., Park, D. A new efficient forest biowaste as biosorbent for removal of
383 cationic heavy metals. *Bioresource Technol.* **175**, 629-632 (2015).
384 25. Su, J., Gao, C., Huang, T., Gao, Y., Bai, X., He, L. Characterization and mechanism of
385 the Cd(II) removal by anaerobic denitrification bacterium *Pseudomonas* sp. H117.
386 *Chemosphere* **222**, 970-979 (2019).
387 26. Ren, Z., Chen, F., Wang, B., Song, Z., Zhou, Z., Ren, D. Magnetic biochar from alkali-
388 activated rice straw for removal of rhodamine B from aqueous solution. *Environ. Eng.*
389 *Res.* **25**, 536-544 (2020).
390 27. Saeed, A., Iqbal, M., Akhtar, M. W. Removal and recovery of lead(II) from single and
391 multimetal (Cd, Cu, Ni, Zn) solutions by crop milling waste (black gram husk). *J. Hazard.*
392 *Mater.* **117**, 65-73 (2005).
393 28. Liu, H., Yang, F., Zheng, Y., Kang, J., Qu, J., Chen, J. P. Improvement of metal
394 adsorption onto chitosan/*Sargassum* sp. composite sorbent by an innovative ion-imprint
395 technology. *Water Res.* **45**, 145-154 (2011).
396 29. Tavares, D. S., Lopes, C. B., Coelho, J. P., Sánchez, M. E., Garcia, A. I., Duarte, A. C.,
397 Otero, M., Pereira, E. Removal of arsenic from aqueous solutions by sorption onto

398 sewage sludge-based sorbent. *Water Air Soil Pollut.* 223, 2311-2321 (2012).
399 30. Agrafioti, E., Kalderis, D., Diamadopoulos, E. Arsenic and chromium removal from
400 water using biochars derived from rice husk, organic solid wastes and sewage sludge. *J.*
401 *Environ. Manage.* **133**, 309-314 (2014).
402 31. Yang, J. S., Kim, Y. S., Park, S. M., Baek, K. Removal of As(III) and As(V) using iron-
403 rich sludge produced from coal mine drainage treatment plant. *Environ. Sci. Pollut. Res.*
404 **21**, 10878-10889 (2014).
405 32. Lee, H., Kim, D., Kim, J., Ji, M. K., Han, Y. S., Park, Y. T., Yun, H. S., Choi, J. As(III)
406 and As(V) removal from the aqueous phase via adsorption onto acid mine drainage
407 sludge (AMDS) alginate beads and goethite alginate beads. *J. Hazard. Mater.* **292**, 146-
408 154 (2015).
409 33. Wang, L., Wang, J. M., Zhang, R., Liu, X. G., Song, G. X., Chen, X. F., Wang, Y., Kong,
410 J. L. Highly efficient As(V)/Sb(V) removal by magnetic sludge composite: synthesis,
411 characterization, equilibrium, and mechanism studies. *RSC Adv.* **6**, 42876-42884 (2016).
412
413
414

Figure legends

Figure 1. Effect of (a) biosorbent shape, (b) chitosan content, (c) sludge content and (d) biosorbent size on adsorption of As(V) on the sludge chitosan (biosorbent dosage = 2 g/L, agitation rate = 200 rpm, contact time = 6 h, temperature = 25 °C, Vw = 200mL, pH non shift(pH 5.5)).

Figure 2. Kinetics of metalloid/metal adsorption (As(V), Cd(II), Cr(VI), and Mn(VII)) onto the sludge chitosan. (biomass dosage = 2 g/L, agitation rate = 200 rpm, contact time = 6 h, temperature = 25 °C, Vw = 200mL, pH non shift(pH 5.5)).

Figure 3. Adsorption isotherms of (a) As(V), (b) Cd(II), (c) Cr(VI) and (d) Mn(VII) by the rod-type biosorbent. The continuous lines were predicted by the Langmuir model; the dotted lines were produced by the Freundlich model. (biomass dosage = 2 g/L, agitation rate = 200 rpm, temperature = 25 °C, Vw = 200mL, pH non shift(pH 5.5))

Figure 1 (a)

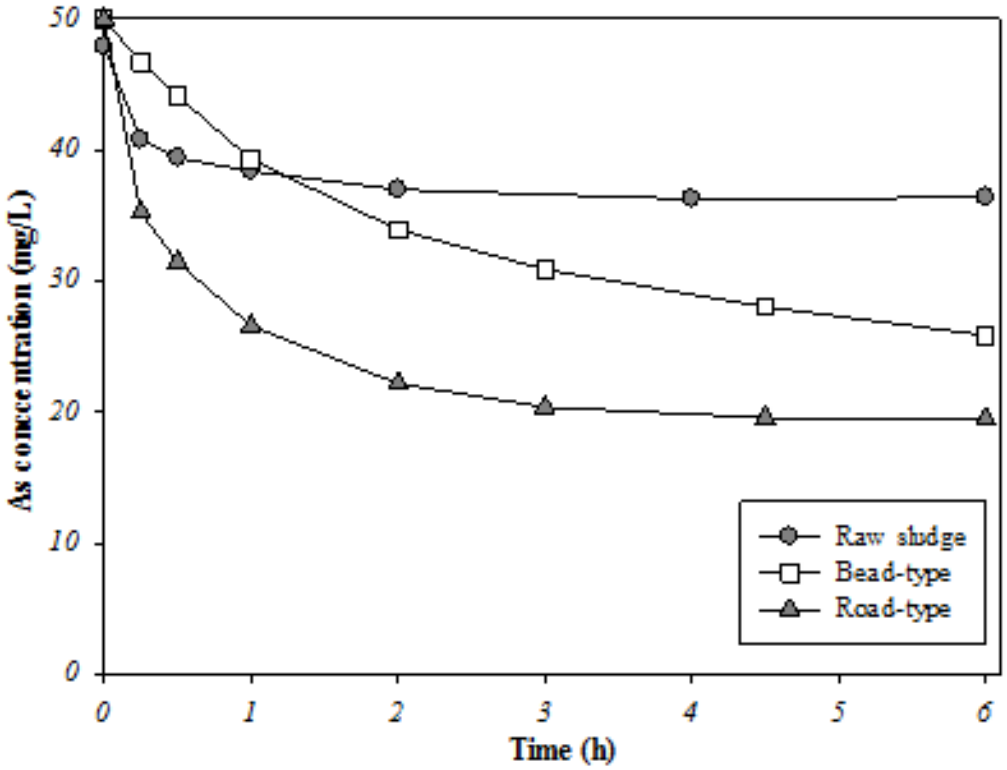
As concentration (mg/L)
Time (h)
Raw sludge
Bead-type
Road-type
0
10
20
30
40
50
0
1
2
3
4
5
6

436 Kim et al Figure 1 (b)

437

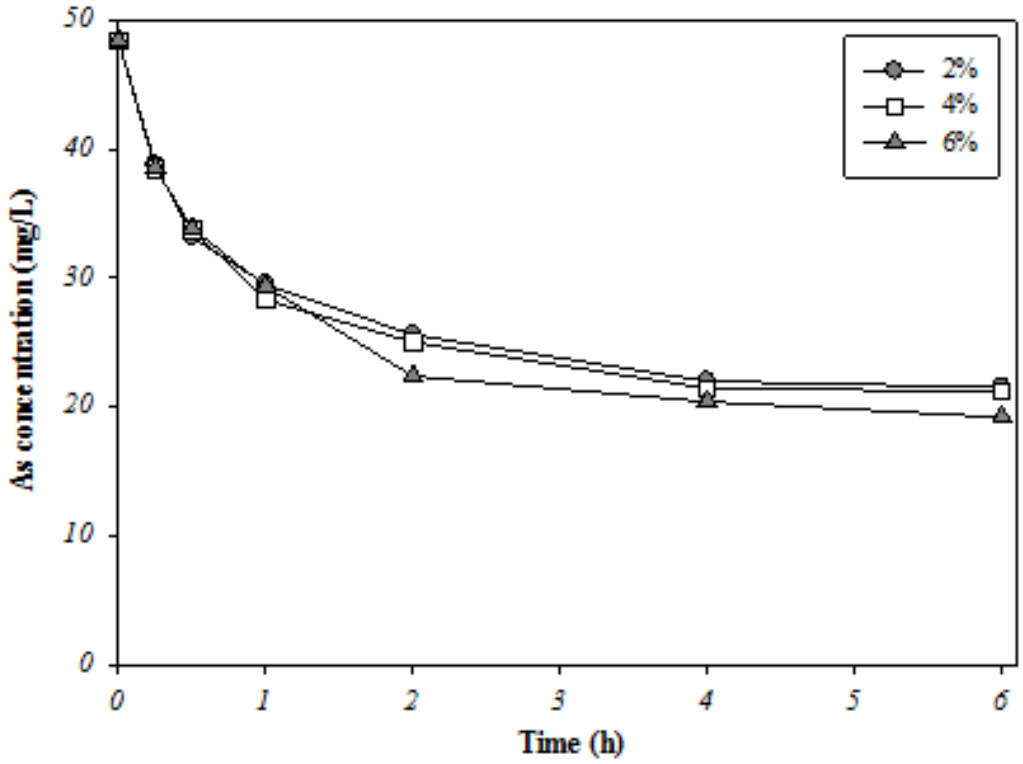

438

439

440

441 Kim et al Figure 1 (c)

442

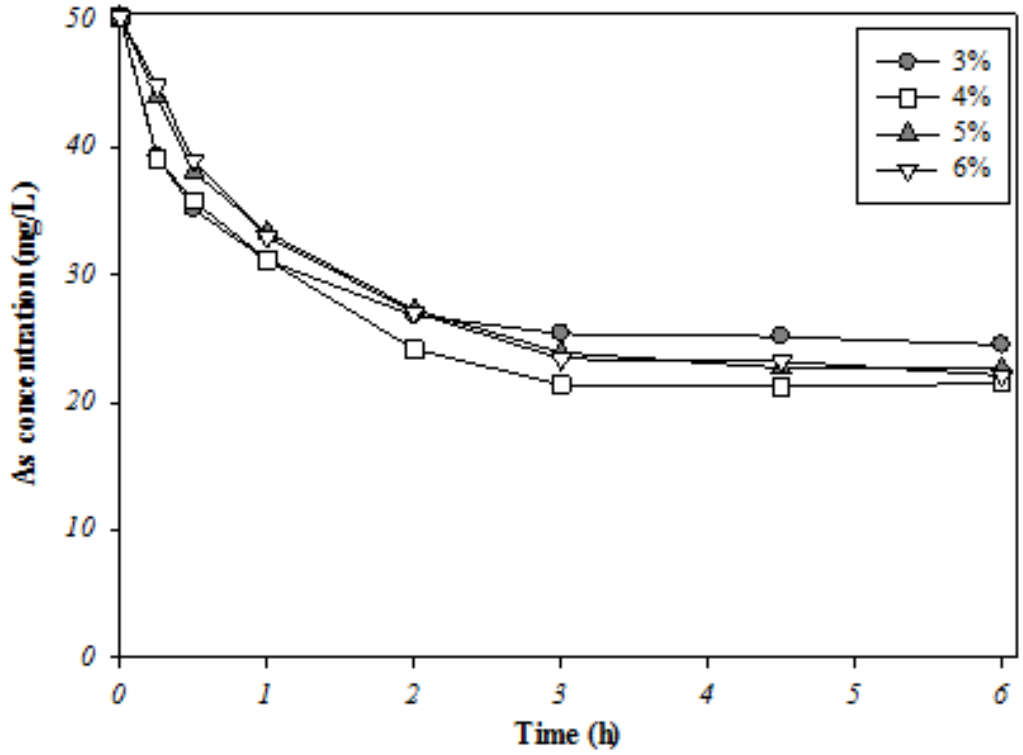

443

444

445

446 Kim et al Figure 1 (d)

447

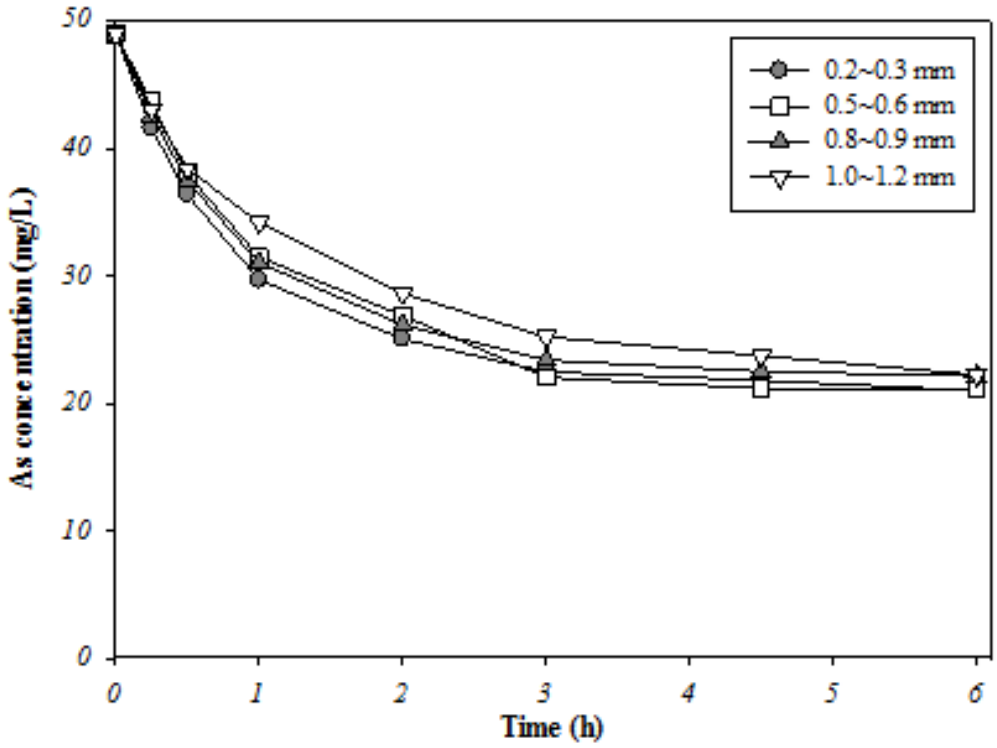

448

449

450

451

453

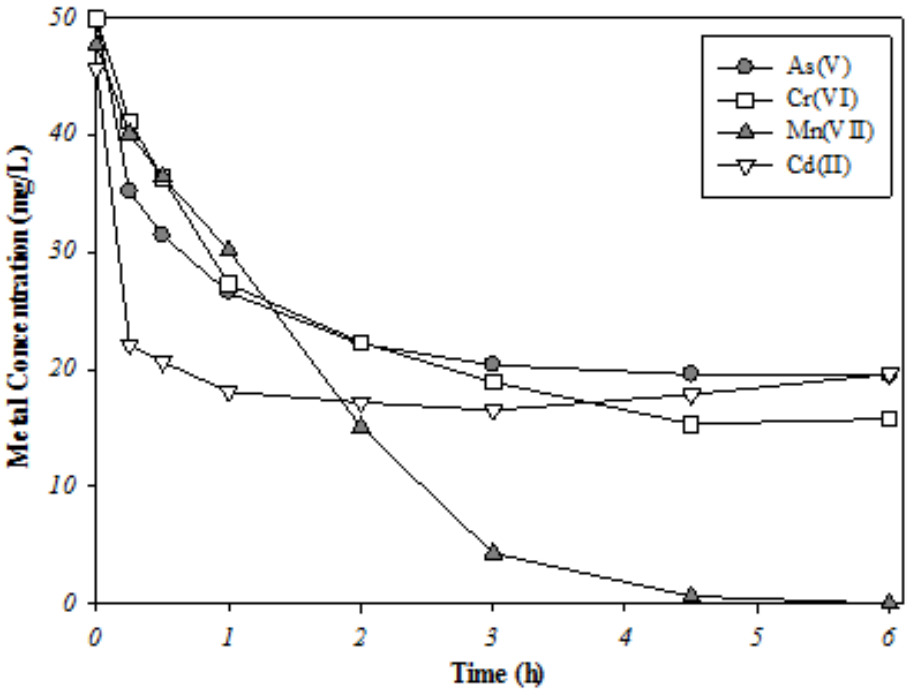

454

455

456

457 Kim et al Figure 3 (a)

458

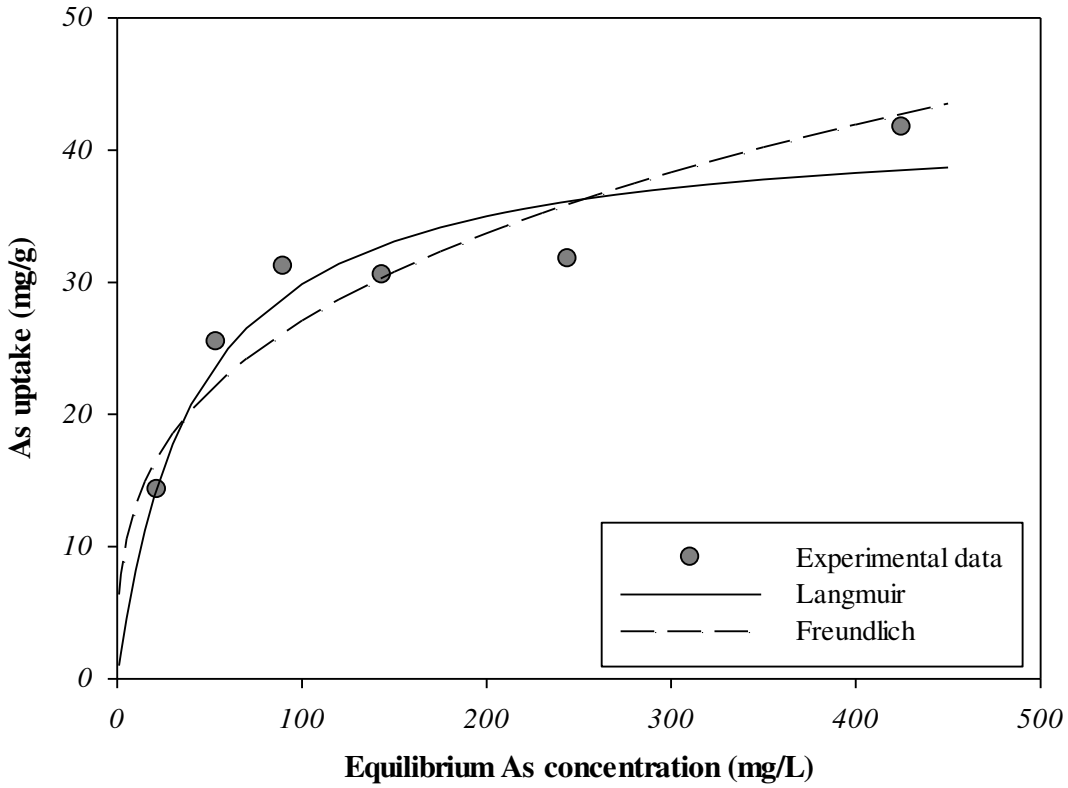

459

460

461 Kim et al Figure 3 (b)

462

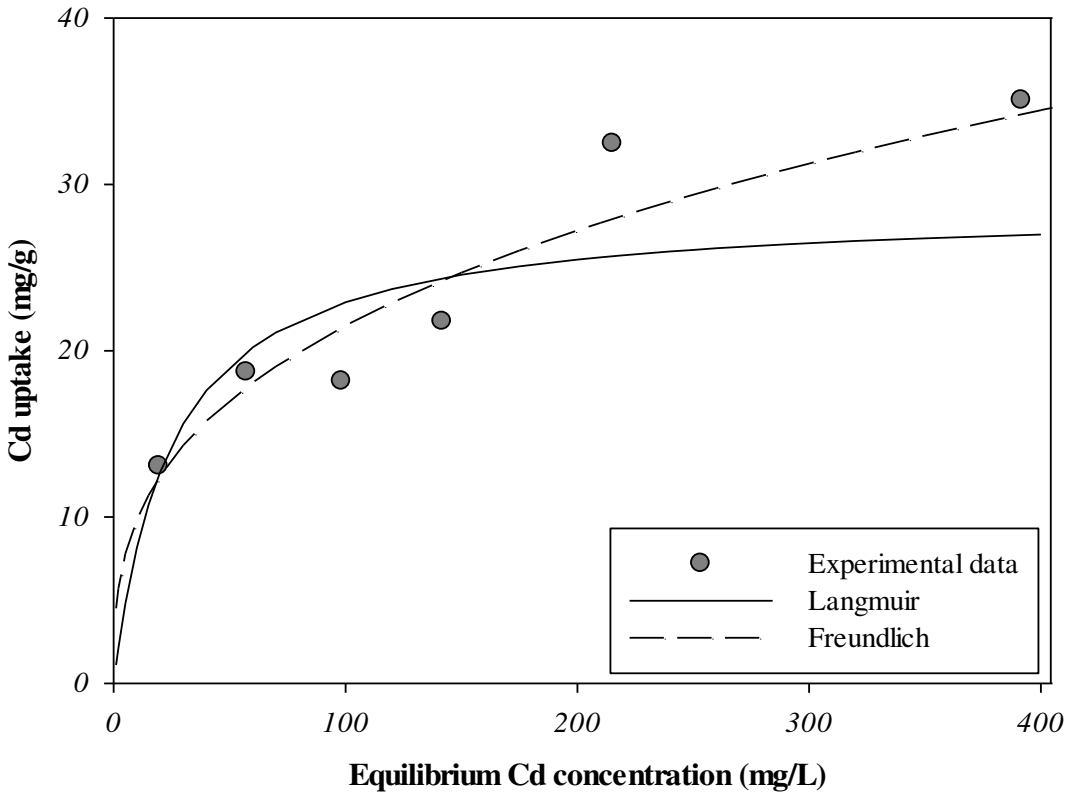

463

464

465

466

467 Kim et al Figure 3 (c)

468

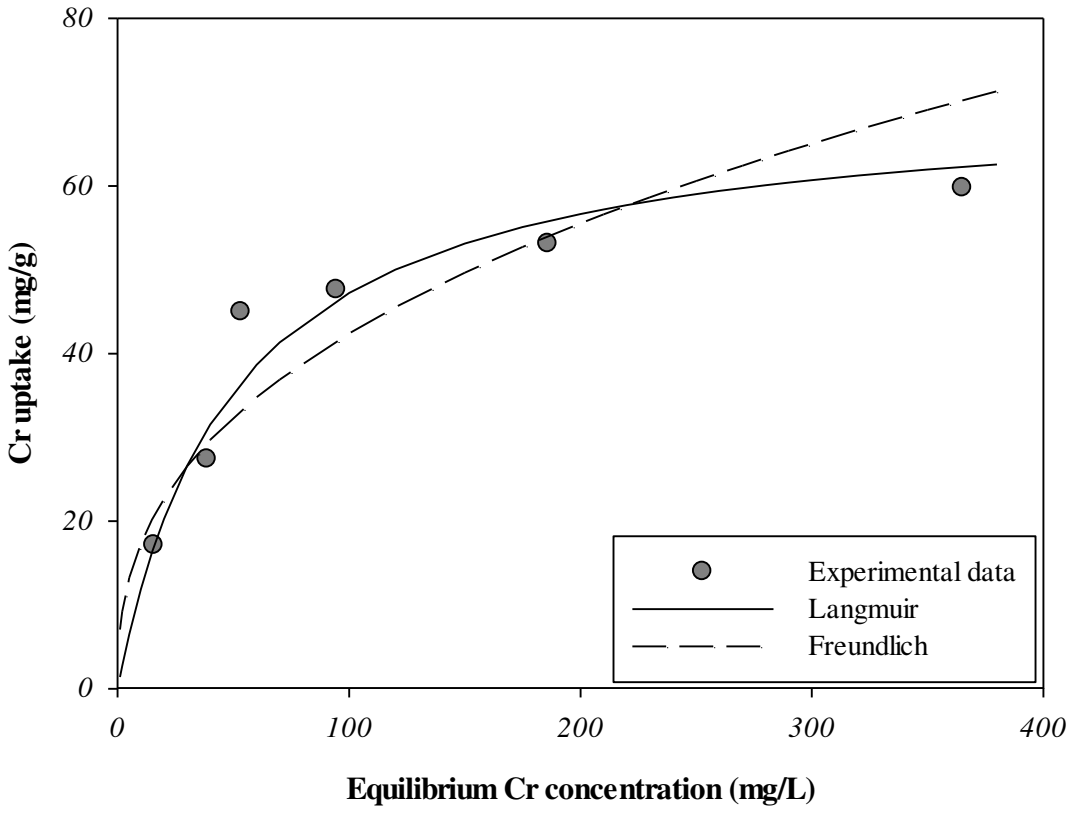

469

470

471

472

473

474

475 Kim et al Figure 3 (d)

476

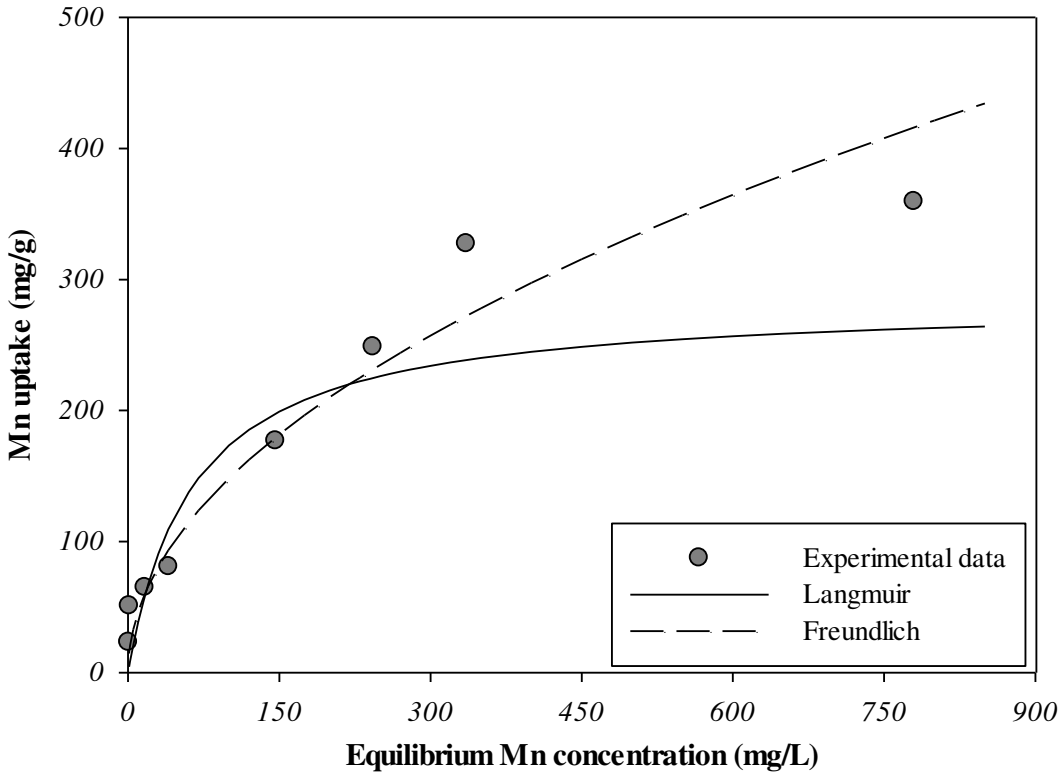

477

478

479

480

481 **Table 1.** Values of TN, TP, TOC and TC released from raw sludge and sludge chitosan.

482

	Biosorbent type	
	Raw sludge	**Sludge Chitosan**
TN (mg-N/L)	30.46	3.60
TP (mg-P/L)	11.63	1.28
TOC (mg-C/L)	26.66	5.02
TC (mg-C/L)	43.77	6.72

483

484

485

Table 2. Comparison of Pseudo-first-order model and Pseudo-second-order model parameter values for different sludge, chitosan content and diameter of the biosorbent

Sludge content (%)	Chitosan content (%)	Diameter (mm)	Pseudo first order			Pseudo second order			
			K_1 (1/h)	q_e (mg/g)	R^2 (-)	K_2 (g/mg·h)	q_e (mg/g)	R^2 (-)	h (mg/g·h)
2.0	**4.0**	**0.2–0.3**	0.96	0.09	0.9889	0.13	14.64	0.9995	28.65
4.0	**4.0**	**0.2–0.3**	1.13	0.08	0.9855	0.14	14.84	0.9995	29.94
6.0	**4.0**	**0.2–0.3**	0.79	0.09	0.9636	0.11	16.08	0.9990	27.33
6.0	**3.0**	**0.2–0.3**	0.84	0.12	0.9395	0.19	13.69	0.9996	35.55
6.0	**4.0**	**0.2–0.3**	1.58	0.06	0.9422	0.10	16.66	0.9956	27.63
6.0	**5.0**	**0.2–0.3**	1.28	0.06	0.9628	0.07	16.16	0.9963	18.48
6.0	**6.0**	**0.2–0.3**	0.78	0.08	0.9475	0.06	16.69	0.9931	16.55
6.0	**4.0**	**0.2–0.3**	0.81	0.09	0.9759	0.09	15.78	0.9984	22.42
6.0	**4.0**	**0.5–0.6**	1.63	0.04	0.9192	0.06	16.82	0.9916	16.13
6.0	**4.0**	**0.8–0.9**	0.95	0.08	0.9969	0.08	15.47	0.9971	19.47
6.0	**4.0**	**1.0–1.2**	0.64	0.08	0.9911	0.06	15.70	0.9992	14.84

492

493 **Table 3.** Kinetic and isotherm constants for the biosorption of As(V), Cd(II), Cr(VI) and

494 Mn(VII) by RCA

495

	Metals	Pseudo first order			Pseudo second order			
		K_1 (1/h)	q_e (mg/g)	R^2 (-)	K_2 (g/mg·h)	q_e (mg/g)	R^2 (-)	h (mg/g·h)
Kinetic	**As(V)**	0.85	8.64	0.9924	0.18	16.21	0.9996	47.68
	Cd(II)	0.51	2.91	0.8452	0.80	14.96	0.9999	178.06
	Cr(VI)	1.33	38.27	0.9840	0.06	19.94	0.9974	23.06
	Mn(VII)	1.02	34.94	0.9642	0.01	34.75	0.9645	14.66
	Metals	**Langmuir**			**Freundlich**			
		Q_{max} (mg/g)	b (L/mg)	R^2 (-)	K_F (mg/g)	n	R^2 (-)	
Isotherm	**As(V)**	42.25	0.0241	0.9711	6.3703	3.18	0.8643	
	Cd(II)	28.69	0.0398	0.8030	4.5064	2.94	0.9048	
	Cr(VI)	70.79	0.0201	0.9648	7.0609	2.57	0.8447	
	Mn(VII)	275.43	0.0163	0.8948	14.1749	1.98	0.9766	

496

497

498

499 **Table 4.** Maximum uptakes of As(V) by various biosorbents manufactured from sludge

500

Sorbent type	Uptake (mg/g)	Experimental condition	Reference
Pyrolysed sludge (Insustry)	0.07	pH 3.0-3.5, 48 h	[29]
Biochar sewage sludge (Domestic)	13.42	pH 6.7-7, 24 h	[30]
Acid mine drainage sludge (Industry)	21.50	pH 7, 24 h	[31]
Acid mine drainage sludge alginate bead (Industry)	21.79	pH 5, 96 h	[32]
Magnetic sludge composite (Domestic)	21.3	pH 2.6, 5 h	[33]
Sludge Chitosan (Domestic)	42.25	pH 5.5, 6 h	This study

501

502

Figures

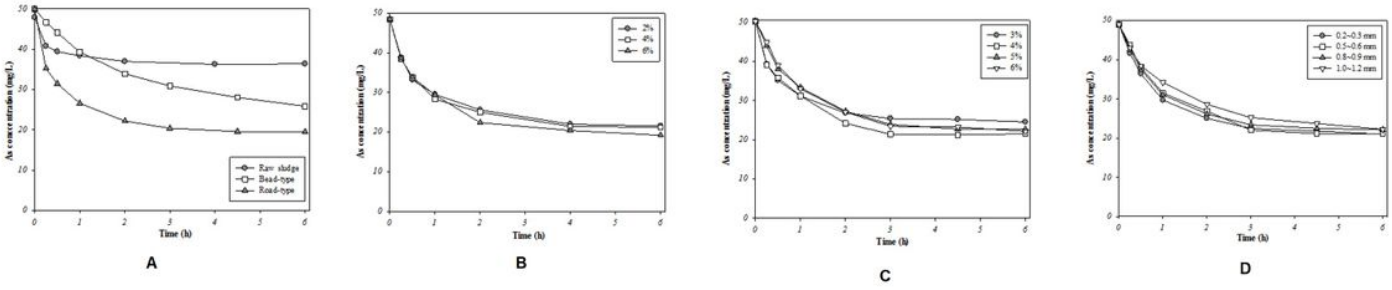

Figure 1

Effect of (a) biosorbent shape, (b) chitosan content, (c) sludge content and (d) biosorbent size on adsorption of As(V) on the sludge chitosan (biosorbent dosage = 2 g/L, agitation rate = 200 rpm, contact time = 6 h, temperature = 25 °C, Vw = 200mL, pH non shift(pH 5.5)).

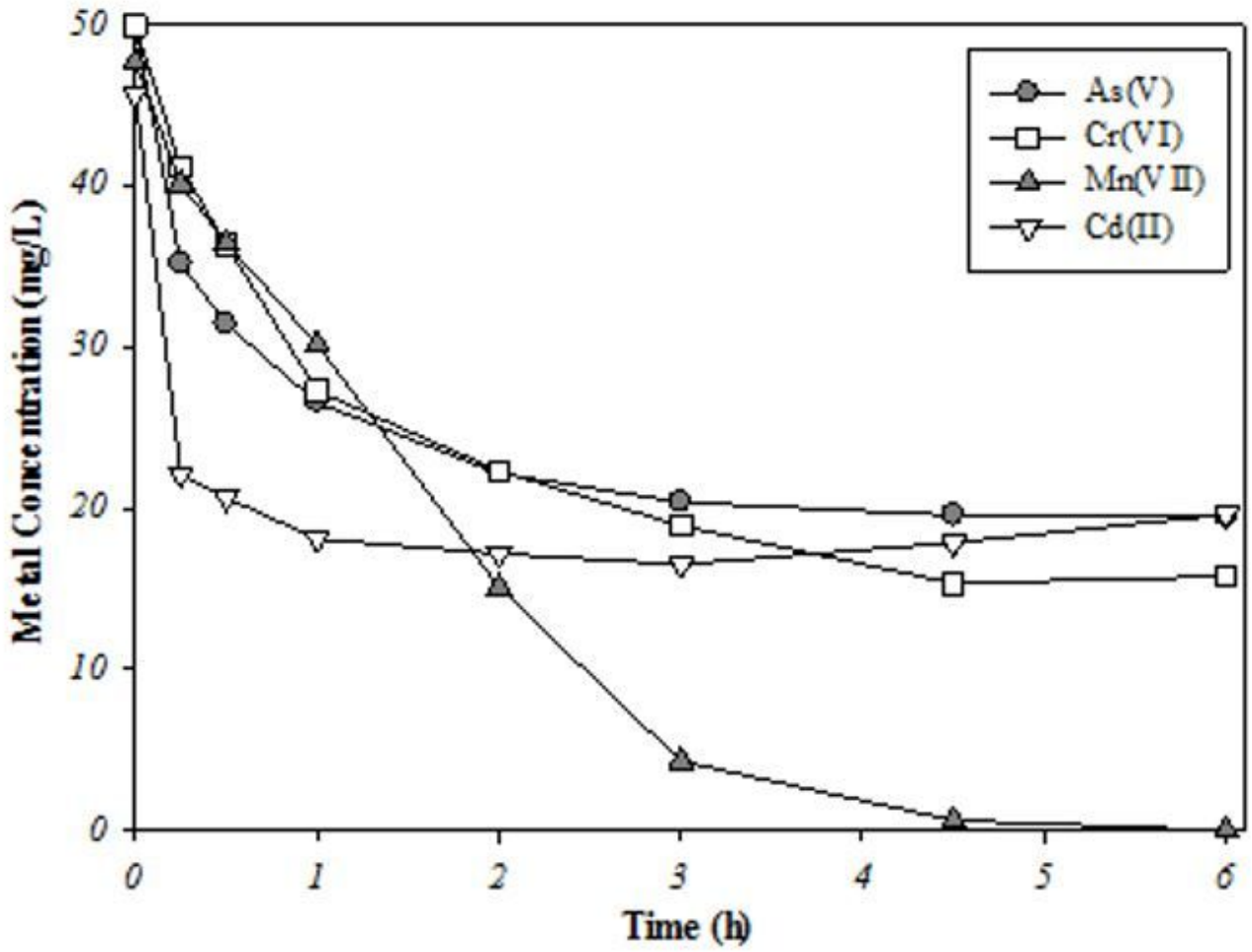

Figure 2

Kinetics of metalloid/metal adsorption (As(V), Cd(II), Cr(VI), and Mn(VII)) onto the sludge chitosan. (biomass dosage = 2 g/L, agitation rate = 200 rpm, contact time = 6 h, temperature = 25 °C, Vw = 200mL, pH non shift(pH 5.5)).

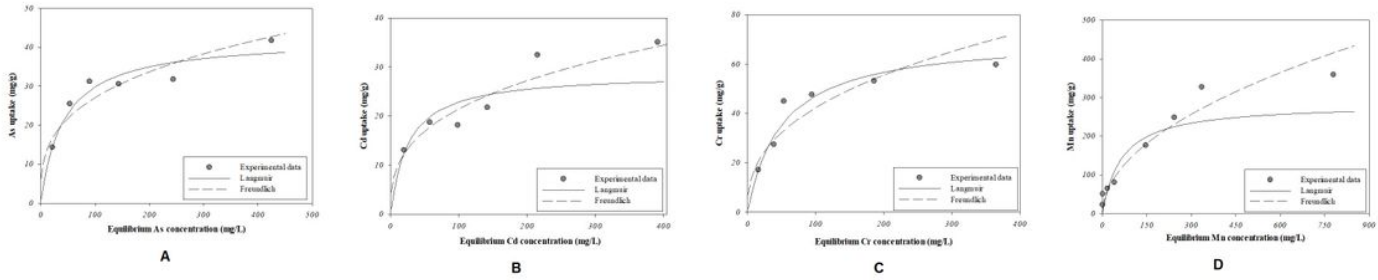

Figure 3

Adsorption isotherms of (a) As(V), (b) Cd(II), (c) Cr(VI) and (d) Mn(VII) by the rod-type biosorbent. The continuous lines were predicted by the Langmuir model; the dotted lines were produced by the Freundlich model. (biomass dosage = 2 g/L, agitation rate = 200 rpm, temperature = 25 °C, Vw = 200mL, pH non shift(pH 5.5))

Supplementary Files

This is a list of supplementary files associated with this preprint. Click to download.

- SupplementaryMaterial.docx